

EFFECTIVENESS OF QUIKSCAT'S ULTRA-HIGH RESOLUTION IMAGES IN DETERMINING TROPICAL CYCLONE EYE LOCATION

Faozi Saïd and David G. Long

Brigham Young University
Microwave Earth Remote Sensing Laboratory
459 Clyde Building, Provo, UT 84602, USA

ABSTRACT

The 25km resolution standard wind products (L2B) are available operationally in near-real time from SeaWinds on QuikSCAT. This relatively low resolution can be enhanced to yield a 2.5km ultra-high resolution (UHR) product that can be used to identify hurricane eye centers more accurately. A comparison is made between the analyst's choice of eye location based on UHR images and interpolated best-track position. In this analysis, the UHR images are divided into two categories based on the analyst's confidence level of finding the eye center location. In each category, statistical error quantities are computed. UHR images within the high-confidence category can provide, for a given year and basin, mean error distance as small as 15km with a 9km standard deviation. The use of these categories may facilitate the realization of QuikSCAT's effectiveness in helping to identify and track hurricane eye centers.

Index Terms— Remote sensing, resolution enhancement, storms, weather forecasting, wind

1. INTRODUCTION

SeaWinds on QuikSCAT is a Ku-band pencil-beam scatterometer capable of accurately estimating wind speed and direction fields over the ocean's surface. It has been consistently operational since July 1999 to the present. Primarily designed for wind observation, SeaWinds is also a tool to analyze tropical cyclones (TCs). However, structural features of TCs may not be easily revealed using standard resolution (L2B) wind products. Thanks to improved resolution [1], these important features (such as TC eye location) may be easily identified using ultra-high resolution images (UHR) instead.

The purpose of this paper is to evaluate the effectiveness of SeaWinds on QuikSCAT in helping identify TC's eye locations using UHR images. The first section briefly describes image rendering, compares ultra-high resolution images versus standard resolution images and introduces a "confidence" metric. The next section presents a short QuikSCAT UHR image analysis for the years 1999 through 2007. Finally, in the last section the reliability of QuikSCAT wind products for TC analysis is discussed by evaluating how often useful data is received in daily analysis.

2. EYE CENTER IDENTIFICATION METHOD

2.1. Image rendering

Standard wind products (L2B and MGDR) available operationally in near-real time are constantly retrieved from SeaWinds on QuikSCAT at 25km resolution. An ultra-high resolution product is also made for

each named TC and is available through the National Environmental Satellite, Data, and Information Service (NESDIS) "manati" Web site (<http://manati.orbit.nesdis.noaa.gov/quikscat/>). For comparison, we use best-track data from the National Hurricane Center (NHC) as well as the Joint Typhoon Warning Center (JTWC) for the five major ocean basins (Atlantic, Indian, South Hemisphere, Western and Eastern Pacific). The data is used to co-locate QuikSCAT passes with TC eye locations. Since best-track data provides eye location only at standard synoptic times for a given TC, a QuikSCAT pass over any TC rarely matches best-track time. To solve this problem, a parametric spline interpolation technique is used to approximate the best-track eye location corresponding to the time of each QuikSCAT pass over a TC.

Two sets of images are eventually created at different resolutions for each given TC within a basin. The first set (L2B) contains wind fields at a standard resolution of 25km, whereas the second set (UHR) is for ultra-high resolution. Each image is manually analyzed to locate the eye center of the TC. Ultimately in this image analysis, our purpose is to compare the error distance between manual eye center location to the best-track position in order to evaluate QuikSCAT's effectiveness in TC analysis.

2.2. Advantages of UHR images over L2B

Standard wind products (L2B) are obtained on a 25x25km grid resolution. In such products, the TC pattern can often be recognized. However, ambiguity selection errors and low resolution can limit the analyst's ability to identify structural features in TCs such as eye center, eyewalls, and other key characteristics.

The AVE algorithm [1] is used to enhance backscatter resolution from a 25km grid to a 2.5km grid from which wind is retrieved. This resolution improvement enables the analyst to identify TC characteristics much faster and easier. To illustrate, the two QuikSCAT images (left and center) in Fig. 1 represent TC Dean in the Atlantic (ATL) basin at 1105 UTC 20 August 2007 at both resolutions. TC characteristics such as eyewall and eye center location are easily identifiable using the UHR image (center) of Fig. 1, whereas it is more difficult to accurately identify them using the lower resolution image (left). Although much more prone to noise and rain contamination [2], UHR images provide more details in the wind speed field compared to L2B images.

2.3. Confidence level with UHR images

Since we have subjectively more confidence in identifying the eye location at higher resolution, UHR image analysis is divided into two categories depending on the confidence level of identifying the

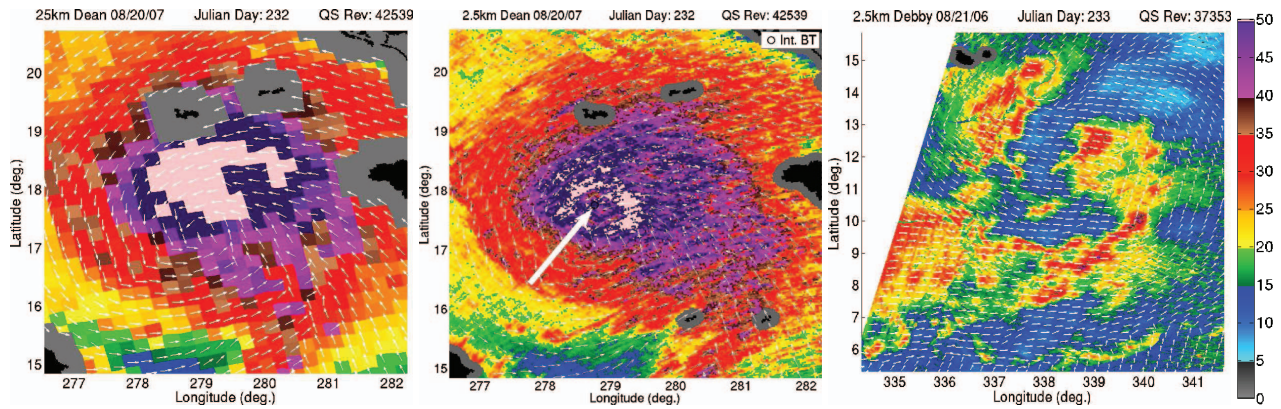


Fig. 1. From left to right: the first two images (L2B and UHR, respectively) show TC Dean in the ATL Basin at 1105 UTC 20 August 2007. The UHR wind speed field on the second image is much more refined (easily recognizable TC characteristics such as eyewall and eye center location) than on the L2B. Note also how the eye location correlates with the interpolated best-track location shown on the UHR image. The third image is TC Debby in the ATL basin at 1913 UTC 21 August 2006. This UHR image is considered a low-confidence case since the eye location (if it exists) is difficult to identify accurately. Note that the wind direction field, represented by white arrows on all three images, is standard L2B winds not UHR. Color scale for wind speed is in knots.

eye in the image. The first category includes images in which we have high-confidence in the eye center location; the second category includes images in which eye center identification is possible but with a low to medium level of confidence. In general, the latter category includes images of under-developed TCs, TCs with equivo- cal wind patterns, TCs half-way over land, or cropped images which only partially cover a TC. The third image (far right) of Fig. 1 shows an early stage of TC Debby in the ATL basin in 2006. This is a good example of an under-developed TC. This UHR image would be considered low-confidence because it is difficult to decide where the eye of the TC is or whether it exists. On the other hand, the second image (center) of Fig. 1 is a good example of what we would consider a high-confidence case. In this particular image, the eye is unambiguously identifiable.

The confidence levels are defined subjectively since the analyst is the one judging whether the eye location is of low or high-confidence. Separating the images into these two categories may be a good way to evaluate QuikSCAT effectiveness in helping identify TC eye locations.

The following subsection is a brief analysis of hurricane season 2003 in the ATL basin where the confidence metric is implemented. All UHR images are first combined then separated into the two confidence categories. Results are then compared using a table containing the standard deviation, mean, and median of the error distance (in kilometers) between our manual eye location and the interpolated best-track eye location. Histograms based on these error distances are plotted and analyzed.

2.4. Implementation of the confidence metric to hurricane season 2003 in the ATL Basin

In 2003, 16 named TCs swept through the ATL basin. For these 16 TCs, 238 UHR and 219 L2B images were analyzed for this particular basin (some of the L2B images were dropped during manual image analysis due to low resolution and lack of pertinent information which helps identify storm's eye location). An error distance histogram is plotted for each set of images (Fig. 2). The error distance represented in this figure is between the interpolated best-track eye

location and the analyst's. By comparing both histograms (first two from the left in Fig. 2), we notice a 40% improvement in the mean error using UHR images over standard resolution images as well as a notable improvement in the median and standard deviation. The UHR images are further analyzed and split into the two confidence categories.

2.4.1. Low and high-confidence categories

The analyst concluded that 84 out of the 238 UHR images for the ATL basin fall in the low-confidence category and 154 in the high-confidence category (see Table 1 for the corresponding statistics). The low-confidence mean error distance is 52km, which is about

Table 1. Statistical results for UHR images (ATL basin-2003)

	Mean (km)	Median(km)	St. dev.(km)
All UHR	32	20	36
Low-Confidence	52	40	53
High-Confidence	21	16	14

60% higher than the mean error for all UHR images combined. Despite the low-confidence criteria given to these images, a high percentage of images (50 out of 84) have an error distance below 50km. Thus, even if the analyst is not sure where the eye location of a TC is, reasonable results are obtained for the eye location for most low-confidence cases. Such results for this category can be very important as forecasters may rely more on microwave sensors than conventional optical images provided by geostationary satellites to track developing storm systems [3].

The mean error distance obtained from the high-confidence set of observations shows a noticeable improvement from both the low-confidence and the overall set of UHR observations. From 32km (all UHR images combined), the mean error for high-confidence decreases to 21km, which is a 35% improvement. Typically, hurricane eyewalls of most developed TCs have a diameter of 30 to 60km [4].

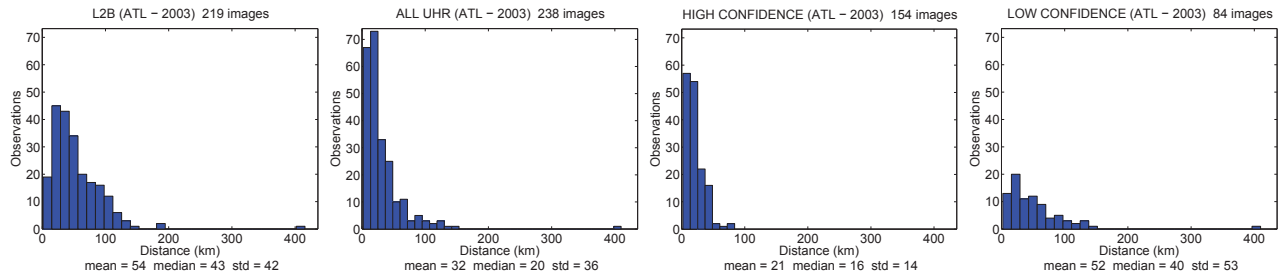


Fig. 2. Error Distance between interpolated best-track eye location and UHR analyst location for all TCs in the ATL basin in 2003. The two most left plots are, respectively, error distance histograms from the L2B images and UHR images. The other two plots show the error distance for the high-confidence images and the low-confidence images. Note that there is a 40% improvement in the mean error using UHR images compared to standard L2B. By splitting the UHR data into these two confidence categories, there is further improvement in the high-confidence mean error distance (all UHR [32km] vs. high-confidence category [21km]). The low-confidence category has a similar mean compared to the L2B image analysis. Axis dimensions are the same for all plots so as to easily compare them.

Thus a 21km mean error for the high-confidence set of observations means that on average the analyst can pinpoint the eye center of a TC within the eyewall. It is interesting to note that for this particular basin and year, high-confidence UHR images represent a fairly large portion (65%) of all UHR images analyzed.

3. QUIKSCAT DATA ANALYSIS FOR THE YEARS 1999 THROUGH 2007

Since the launch of QuikSCAT (19 June 1999) up through 2007, a total of 1719 relevant UHR images from SeaWinds have been generated for TC analysis in the ATL and Eastern Pacific (EP) basins. Additionally, SeaWinds on ADEOS II (launched 14 December 2002, failed 24 October 2003) provided another 193 relevant UHR images for the year 2003. The confidence metric is used to categorize the images and yearly error distance results are derived and compared for each basin.

3.1. The ATL Basin

For the ATL basin, the low and high-confidence categories encompass, respectively, 424 and 601 UHR images. Figure 3 shows a table (upper left) with the mean error distance, median, and standard deviation, as well as the number of low/high-confidence observations for each year (1999 to 2007). The corresponding error plot (bottom left of Fig. 3) shows a fairly small and consistent average in the error distance of the TC eye position; for the low-confidence set of images, the mean varies between 50km and 70km, while the high-confidence mean varies between 15km and 25km. We assume from the latter results that the analyst was able to identify most (if not all) eye center locations of all TCs (within the high-confidence category) in the ATL basin between 1999 and 2007. Since 601 out of 1025 UHR images are part of the high-confidence category, eye center locations were accurately determined for about 59% of all UHR images in this basin.

3.2. The EP basin

UHR images obtained from SeaWinds provide very similar results for the EP basin though with fewer images. The low and high-confidence categories contain, respectively, 363 and 524 relevant UHR images (versus 424 and 601 for the ATL basin). Statistical

results for these categories are also found in Fig. 3 with the corresponding error plot (right). The results for the EP basin are similar to the ATL except that the yearly mean and the standard deviation for the low-confidence category are on average lower. As for the high-confidence category, we obtain very consistent results with a yearly mean around 24km. This means that the analyst was able to find the TC eye location in almost all high-confidence UHR images for this particular basin. This is very promising and helps demonstrate the effectiveness and reliability of QuikSCAT UHR images to help find TC eye location simply by relying on the wind speed field.

4. QUIKSCAT OBSERVATIONS RELIABILITY

A key question for QuikSCAT data utility is how often SeaWinds wind products are available for cyclone tracking. The QuikSCAT satellite is in a polar orbit and revolves around the globe in approximately 101 minutes. With an 1800km swath, it is capable of measuring the normalized radar backscatter from 90% of the planet twice in 24 hours. In the areas where most TCs occur, at most two observations per day are available (in some rare locations such as the Gulf of Mexico, up to three times). Thus, when tracking a TC it may be possible to obtain two UHR images from QuikSCAT daily. However, eye locations may not always be identifiable in every image; at times TCs may be only partially covered, part-way over land, or in an under-developed stage. Such images may not be useful for TC analysis. As a result, UHR images useful in determining the eye location of a given TC range from zero to two in a given day.

A pie chart for each basin (see Fig. 4) shows the distribution of useful UHR images received daily (results combine years 1999 through 2007). The ideal situation is to obtain two useful QuikSCAT observations per day all the time; however this occurred only 25.7% and 19.1% of the time in the ATL and the EP respectively (see Fig. 4). Nevertheless, at least one useful UHR image is obtained daily 60.5% (ATL) and 76.7% (EP) of the time. Having at least two scatterometers on different platforms in polar orbits would improve the results. Judging the usefulness of an image is a subjective task and relies heavily on the analyst's experience of interpreting a QuikSCAT wind fields UHR image. Therefore, it may be possible that the usefulness of images may be higher than reported here.

ATL basin	99	00	01	02	03	04	05	06	07	EP basin	99	00	01	02	03	04	05	06	07
LC Mean (km)	70	61	60	57	52	70	50	66	49	LC Mean (km)	40	43	67	52	54	71	48	50	42
LC Med. (km)	44	52	38	42	40	54	53	56	45	LC Med. (km)	28	38	51	52	50	62	43	41	35
LC Stdv. (km)	69	53	64	54	53	70	36	46	36	LC Stdv. (km)	35	23	51	31	32	46	38	38	26
Total LC obs.	38	31	43	27	84	31	44	78	48	Total LC obs.	13	26	31	25	91	36	25	84	32
HC Mean (km)	18	24	25	24	21	19	23	15	24	HC Mean (km)	25	27	26	25	24	23	25	21	24
HC Med. (km)	13	21	23	19	16	15	21	16	18	HC Med. (km)	21	24	21	24	20	21	20	16	20
HC Stdv. (km)	15	19	15	17	14	16	15	9	17	HC Stdv. (km)	17	20	15	12	14	14	20	22	14
Total HC obs.	42	60	55	42	154	76	115	32	25	Total HC obs.	35	59	52	49	80	59	72	77	41

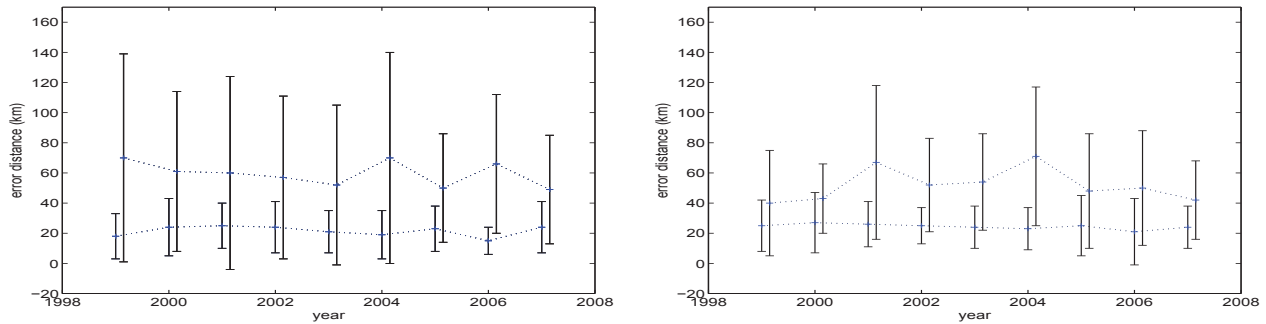


Fig. 3. Statistical results for low/high-confidence UHR images in the ATL (left) and EP (right) basins for the period 1999-2007. The tables provide yearly mean, median and standard deviation (in kilometers) for each confidence category for the difference between analyst manual eye locations and interpolated best-track eye locations. The corresponding plots show yearly means and their respective standard deviations for each basin. The curves with lower means (around 20-25km) correspond to the high-confidence category while the others with larger means to the low-confidence category.

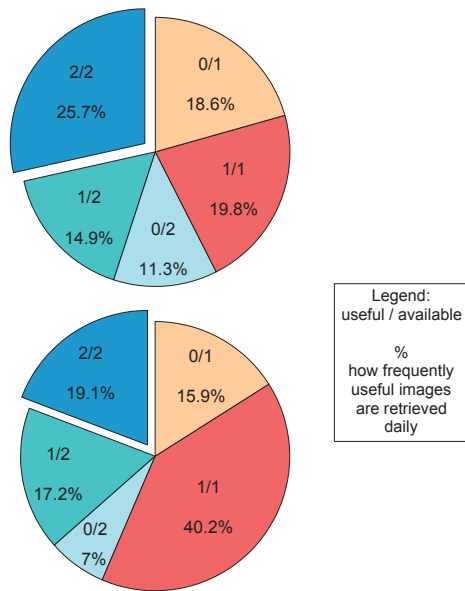


Fig. 4. Pie charts displaying how often useful UHR images are retrieved for TCs of all QuikSCAT images available daily, as noted on each slice (top: ATL and bottom: EP; years 1999-2007 combined). Up to two images can be retrieved per day though in many cases only a single image per day is available. The exploded slices show that two useful (for TC eye identification) out of two available images per day were obtained for 25.7% (ATL) and 19.1% (EP) of the time between 1999 and 2007.

5. CONCLUSION

Though prone to noise and rain contamination, the 2.5km ultra-high resolution images from SeaWinds on QuikSCAT reveal mesoscale features which are not visible in standard 25km wind fields. Thus, UHR images can be used to identify more easily and accurately TC eye locations. Poor results may still be obtained at times. However, these are mostly due to under-developed TC stage or to the analyst's capability to identify TC characteristics. By dividing the UHR images into two categories based on the analyst's confidence level of finding the eye center location, the realization of QuikSCAT's effectiveness in helping to identify these critical locations may be more evident.

6. REFERENCES

- [1] J.B. Luke D.G. Long and W. Plant, "Ultra high resolution wind retrieval for SeaWinds," in *International Geoscience and Remote Sensing Symposium*, Toulouse, France, July 2003, pp. 1264-1266.
- [2] D.G. Long, "Ultra high resolution rain retrieval from QuikSCAT data," in *International Geoscience and Remote Sensing Symposium*, Denver, Colorado, August 2006, pp. 4113-4116.
- [3] P. Chang W. Timothy Liu K.B. Katsaros, E.B. Forde, "QuikSCAT's SeaWinds facilitates early identification of tropical depressions in 1999 hurricane season," *Geophysical research letters*, vol. 28, no. 6, pp. 1043-1046, March 2001.
- [4] C. Weatherford and W. M. Gray, "Typhoon structure as revealed by aircraft reconnaissance. Part II: Structural variability," *Monthly Weather Review*, vol. 116, pp. 1044-1056, 1988.